FISEVIER

Contents lists available at ScienceDirect

# Solid State Electronics

journal homepage: www.elsevier.com/locate/sse



# A comprehensive analysis of Auger generation impacted planar Tunnel FETs

Sheikh Z. Ahmed<sup>a,\*</sup>, Daniel S. Truesdell<sup>a</sup>, Yaohua Tan<sup>b</sup>, Benton H. Calhoun<sup>a</sup>, Avik W. Ghosh<sup>a,c</sup>



- <sup>a</sup> Department of Electrical and Computer Engineering, University of Virginia, Charlottesville, VA 22904, USA
- <sup>b</sup> Synopsys, San Jose, CA, USA
- <sup>c</sup> Department of Physics, University of Virginia, Charlottesville, VA 22904, USA

#### ARTICLE INFO

The review of this paper was arranged by "A. Zaslavsky"

#### ABSTRACT

Tunnel Field Effect Transistors (TFETs) are known to be compromised by higher order processes that downgrade their performance compared to ballistic projections. Using a quasi-analytical model that extends the chemistry based Simmons equation to include finite temperature effects, potential variations and scattering, we exhibit that non-idealities like trap-assisted tunneling and Auger generation can explain the observed performance discrepancy. In particular, Auger generation is the dominant leakage mechanism in TFETs at low trap densities. Our studies suggest that possible ways of reducing Auger generation rate are reducing source carrier concentration and increasing the valence band transport effective mass of the source material. In this paper, we specifically investigate the impact of variations of these factors on device performance of staggered bandgap planar III-V heterojunction Tunnel FETs.

### 1. Introduction

Computing in the post-Moore's law era is now increasingly reliant on novel architecture rather than simply improving switching devices. Nonetheless, increasing the energy efficiency of electronic switching remains a critical goal, especially for embedded Internet of Things applications. The scalability of complementary metal oxide semiconductor (CMOS) devices is constrained by the fundamental Boltzmann limit on its switching voltage. Boltzmann physics limits the Subthreshold Swing (SS) to  $k_B T ln 10/q \sim 60 \text{ mV/decade}$  at room temperature, which sets the steepness of the MOSFET gate transfer characteristic in the subthreshold region [1]. The resulting power dissipation poses a major bottleneck for further scaling of CMOS devices [2]. Novel transistor architectures like Tunnel FETs (TFETs) [3], Graphene Klein Tunnel FETs [4], Nanoelectromechanical FET [5], Mott transition based Hyper FET [6] and Negative Capacitance FET [7] have been proposed, which propose unconventional switching to bypass the Boltzmann limit.

Among all the proposed sub-Boltzmann devices, TFETs are the most widely studied and have shown excellent theoretical results. Some experimental tunnel transistors have demonstrated below 60 mV/decade but for extremely low currents [8,9]. However, the low SS of TFETs cannot be sustained for at least four orders of magnitude of current required for driving logic circuits, nor is the low current adequate for speed and drivability. Previous attempts to increase the ON current

with heterojunction Type-II staggered gap engineering while keeping the SS low have not been completely successful [10,11]. More recently there have been reports of some III-V TFETs which have SS < 60 mV/decade for two to three orders magnitude of current in the 1–100 nA/ $\mu m$  range, which is significantly lower than the ON current of state of the art transistors [10,12–15]. It is therefore imperative to understand the limiting processes in TFETs and calibrate with experiments, thereby identifying ways to minimize these processes in order for further improvement in device performance.

Reports from some earlier simulations suggest that traps and Auger generation are the two major leakage mechanisms restricting TFET performance [16,17]. We recently developed a chemistry based quasianalytical model for planar ultra-thin body TFETs that includes these non-idealities [18]. Ultra-thin bodies offer better electrostatic control in comparison to their bulk counterparts. It is well known that reducing trap densities in heterojunction TFETs is essential to avoid band realignment and band-to-band tunneling, and experimentalists have been focusing on that front. However, even in the absence of traps, the TFET OFF current is not reduced to levels predicted by ballistic simulations. In this limit Auger processes raise the current floor and limit SS as a result. There is no detailed study on diminishing the effect of Auger generation, present even in the absence of traps, especially for the abrupt staggered band offsets needed otherwise for high ON current. It is thus necessary to determine the important factors affecting Auger generation and how altering those affect the steepness of the transfer

E-mail address: sheikh.ahmed@virginia.edu (S.Z. Ahmed).

<sup>\*</sup> Corresponding author.

Fig. 1. (a) Simulated planar double gate GaSb/InAs heterojunction TFET structure. (b) Auger generation process, where source valence band electrons collide with hot holes which gives them sufficient energy to move to the channel conduction band.

characteristic.

In this work, we identify the source carrier concentration and source valence band transport effective mass as the two main determinants of Auger generation. In Section 2, the quasi-analytical model used for our simulations is briefly described. The effects of the aforementioned factors on OFF current, ON current and subthreshold swing are discussed in Section 3.

#### 2. Simulation method

In this letter, we study the characteristics of a n-type double gated GaSb/InAs heterojunction TFET using our quasi-analytical model. The TFET structure is shown in Fig. 1(a). The source, channel and drain doping concentrations are  $N_S$ ,  $N_{ch}$  and  $N_D$  respectively. The channel thickness is  $t_{ch}$  and oxide thickness is  $t_{cx}$ . The source, channel, drain and oxide dielectric constants are  $\epsilon_S$ ,  $\epsilon_{ch}$ ,  $\epsilon_D$  and  $\epsilon_{ox}$  respectively. The GaSb/InAs based source/channel junction forms a type-II heterojunction which permits interband tunneling without a barrier.

## 2.1. Ballistic current model

Accurate band and surface potential models are required for computing the tunneling probability of electrons in the TFET structure. A 2-band k. p model is used to simulate the real and imaginary bands of the materials [18]. This model is fitted to tight binding results that are calibrated to Density Functional Theory (DFT) band structure and wavefunctions [19,20]. A pseudo-2D Poisson's equation is solved to obtain the surface potential in the planar device [18]. The surface potential can be utilized for both homojunction and heterojunction TFETs.

For computing the band-to-band tunneling (BTBT) current the k-vectors are calculated from the band and surface potential models. A modified Simmons equation is then employed to calculate current. The Simmons model is well known in chemistry for quantitatively approximating the WKB (Wentzel-Kramers-Brillouin) current through the multiple modes in a thin film [21]. Simmons performed a Taylor expansion on the barrier profile in the WKB exponent around a rectangular barrier and then summed over a series of transverse modes. In our quasi-analytical model, the Simmons equation is modified to work for non-rectangular barriers. It also accounts for effects of finite temperature which determines the subthreshold swing for switching. Our modified Simmons equation arises from a Landauer formalism

$$I = \frac{q}{h} \int T(E) [f_S(E) - f_D(E)] dE$$
(1)

Here, T(E) gives the total transmission summed over all the transverse states at a particular energy. The source and drain Fermi-Dirac functions,  $f_S(E)$  and  $f_D(E)$ , set the approximate room temperature energy window for the tunneling electrons.

## 2.2. Trap assisted tunneling

The high mobility of III-V materials can be advantageous for nanoscale devices, but their performance is limited by high trap densities at the material interfaces. These traps arise due to the lattice and valency mismatch of the different materials. Due to these traps, intermediate energy levels are created inside the bandgap that can be occupied by carriers. Electrons in the source valence band can jump to the channel conduction band via one of these trap states through a multiphonon process. This unwanted mechanism creates a leakage path in the OFF state of the TFET which leads to detrimental effects like higher OFF current and higher SS in the subthreshold region. In our model we consider the trap assisted tunneling process as a type of Fowler-Nordheim tunneling through a tilted barrier around the trap. The trap current per unit width,  $I_{TAT}$ , is written in the following compact form [22]

$$I_{TAT} = \frac{q}{2} v_{rcmb} n_i \Gamma d \left[ 1 - e^{-qV_{DS}/k_B T} \right], \tag{2}$$

where  $\Gamma$  represents the electric field enhancement due to the trap assisted tunneling and thermionic emission process and d represents the trap active region,  $n_i$  is the intrinsic carrier concentration in the source and  $V_{DS}$  is the drain-to-source voltage drop. The recombination velocity  $v_{remb} = \sigma v_{th} N_t$  and  $\int D_{it} dE = \int N_t \delta(E - E_i) dE = N_t$ . Here, the trap density per unit area at the midgap energy is given by  $N_t$ , while  $D_{it}$  converts this into a density of states with a delta function profile at the trap energy. We consider only midgap trap density since they have the highest probability of being occupied by electrons undergoing TAT.

## 2.3. Auger generation

Even for nearly pristine interfaces with low trap densities, the high electric field near the source/channel junction can trigger another leakage path by means of the Auger generation process [23]. This is an intrinsic mechanism which involves charge scattering through Coulomb interactions. In Auger generation three particles are involved where a "hot" carrier collides with a valence band electron causing it to move to the conduction band, as shown in Fig. 1(b).

Since the ON current of TFETs is also driven by tunneling, the use of staggered bandgap heterojunctions in the source/channel region has been proposed to increase the ON current to acceptable values. This results in a steep narrow junction which generates a high electric field, leading to increased tunneling probability in the ON state. In the OFF state, this narrow junction increases the overlap between the valence band and conduction band wavefunctions. Through this interaction extra holes are generated in the valence band and extra electrons in the conduction band through Auger processes. Auger generation does not have a significant impact on the ON state BTBT current. However, it significantly increases the OFF state current which becomes a limiting factor for the subthreshold slope in TFETs. The Auger generation rate is

S.Z. Ahmed. et al. Solid State Electronics 169 (2020) 107782

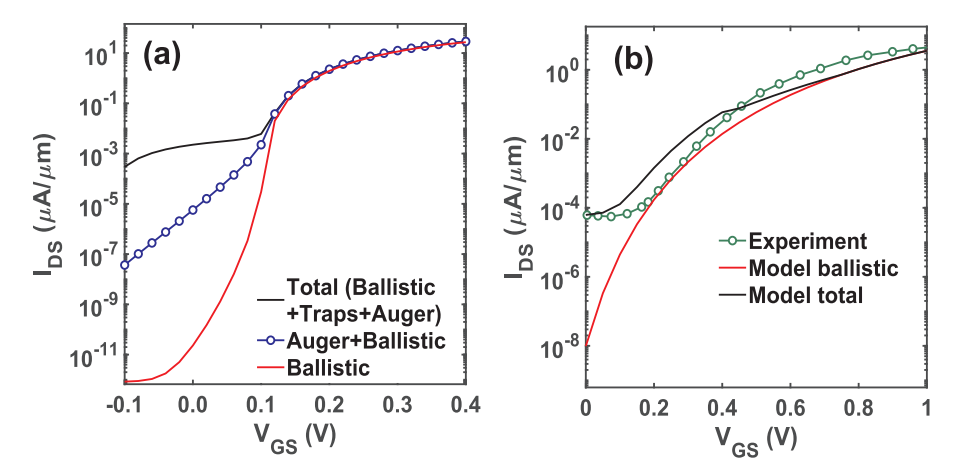


Fig. 2. (a) Comparison of non-ideal currents with ballistic current for a heterojunction TFET simulated using our model. Ballistic current has a steep switching, Auger increases OFF current and Subthreshold Swing. TAT dominates over others. Here we use  $D_{lt} = 5 \times 10^{12}$  cm<sup>-2</sup> eV<sup>-1</sup> which is consistent with current InAs-oxide trap densities [25]. (b) Model calibration with experimental homojunction InGaAs TFET at  $V_{DS} = 0.3$  V [24].

approximated by employing Fermi's Golden Rule [18,23]

$$G = \frac{1}{A} \frac{2\pi}{h} \sum_{1,1',2,2'} P(1, 1', 2, 2')$$

$$|M|^2 \delta(E_1 - E_{1'} + E_2 - E_{2'}). \tag{3}$$

As illustrated in Fig. 1 correspond to initial states, while 1' and 2' correspond to final states in Auger generation mechanism. The P is the occupancy of the initial and final states, given by

$$\begin{split} &P_{HCHH}(1, 1', 2, 2') \\ &= \bar{f}_{\nu}(E_1)\bar{f}_{\nu}(E_2)f_c(E_1)f_{\nu}(E_2) - f_{\nu}(E_1)f_{\nu}(E_2)\bar{f}_c(E_1)\bar{f}_{\nu}(E_2) \approx \bar{f}_{\nu}(E_1)\bar{f}_{\nu}(E_2) \\ &f_c(E_1) - \bar{f}_{\nu}(E_2) \end{split} \tag{4}$$

where  $\bar{f}=1-f$  is the hole occupancy. The subscripts allude to the bands involved in the process, heavy-hole and conduction band.

## 3. Results and discussion

We simulate a double gated III-V heterojunction tunnel FET with GaSb as the source and InAs as the channel/drain. The simulated transfer characteristics of the TFET are shown in Fig. 2a) and calibration of the model with a fabricated InGaAs homojunction TFET in Fig. 2(b) [24]. The calibrated model marginally overestimates the current in the subthreshold region and underestimate the ON current at some voltages. The effect of non-idealities on the characteristics are shown in the figure. Significantly, even in the absence of traps at perfect

interfaces, Auger generation causes a significant increase in the OFF current and SS. While a high ON current requires steep band variations to thin the tunnel barrier, the resulting large electric fields push up Auger generation, bringing up the OFF current at the same time. Increasing trap density further compromises the overall OFF current. For fitting the experimental results a trap density of  $10^{11} \, \mathrm{cm^{-2}eV^{-1}}$  is used. In order to fit the data more accurately (in the linear scale), we multiply a fitting factor of 0.5 to the Auger generation current to account for non-idealities, like Coulomb screening, that has not been considered in this model. In VLSI circuits, the ON and OFF voltages are generally defined relative to the ground (0 V) and power supply voltage ( $V_{DD}$ ), respectively. Following this convention, in our simulations, we define  $I_{OFF}$  to be the current at  $V_{GS} = 0V$  and  $V_{DS} = V_{DD}$  and  $I_{ON}$  to be the current at  $V_{GS} = V_{DD}$ .

In addition to minimizing traps, the reduction of other leakage mechanisms like Auger generation is critical to realizing steep transfer characteristics. The Auger process strongly depends on the carrier concentration and material effective mass. The source doping,  $N_S$ , determines the number of electrons available to participate in the Auger generation process, while the valence band (VB) effective mass controls the wavefunction confinement and hence the wavefunction overlap between the valence and conduction band states that enter the scattering matrix element M [18,23]. We study the effect of changing these parameters on  $I_{OFF}$ ,  $I_{ON}$  and on/off ratio in the absence of the TAT component. For these simulations we consider a channel length  $L_{ch} = 100$  nm, channel thickness  $t_{ch} = 5$  nm and oxide thickness

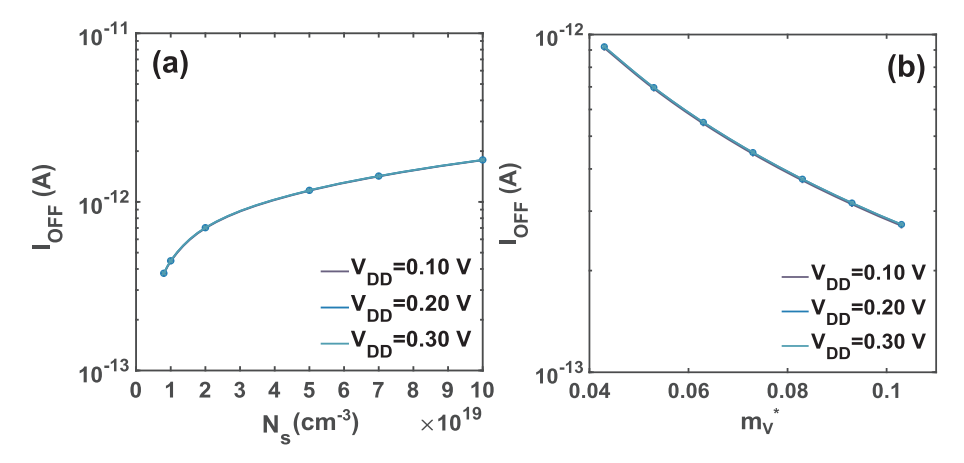


Fig. 3. OFF current (including Auger Generation) vs. (a) source carrier concentration (b) source valence band effective mass for simulated double gate TFET, in the absence of traps ( $N_t = 0$ ), with parameter values from our previous paper [18].

 $t_{ox} = 2 \text{ nm}.$ 

S.Z. Ahmed, et al.

The relationship between  $I_{OFF}$  and  $N_S$  is shown in Fig. 3(a). The off current increases by nearly an order of magnitude when source doping is increased by a similar number. The increased carrier concentration increases the probability of collision which leads to a higher Auger generation rate. The OFF current decreases by a factor of 4.5 if  $N_S$  decreases from  $1 \times 10^{20} \, \text{cm}^{-3}$  to  $8 \times 10^{18} \, \text{cm}^{-3}$ . The VB effective mass dependence of the off current is shown in Fig. 3(b) assuming the material bandgap remains unchanged. For our simulations we consider the hole transport effective mass. Heavy-hole bands in III-V materials are known to be strongly anisotropic and in ultra-thin bodies, such as ours, the 2D hole subband structure strongly depends on the confinement plane [26,27]. Long et al. have stated that for a 2 nm thick p-GaSb/n-InAs TFET the hole transport effective mass is 0.073  $m_0$  given (110) confinement and [110] transport [28]. Due to this confinement, the heavy hole effective mass decreases and becomes comparable to the light-hole effective mass. It is observed that increasing  $m_v^*$  leads to a reduction in the OFF current. This happens because as the mass increases the wavefunction of the valence electrons gets more confined in real space. This leads to an overall reduction in wavefunction overlap between the valence band and conduction band states, thus reducing  $I_{OFF}$ . The valence band transport effective mass approaches the bulk heave hole effective mass if the channel thickness is increased. We expect that in this regime the Auger generation will exhibit similar dependence on the effective mass. However, increasing the channel thickness to bulk values will adversely effect the electrostatic control of the gate. This will negatively impact the band-to-band tunneling and result in degraded performance of the TFET.

Fig. 4(a) and (b) exhibit the ON current dependence on the source doping and VB effective mass. In Fig. 4(a) it is observed that  $I_{ON}$  increases with doping concentration at low supply voltage,  $V_{DD}$ . For high supply voltages the ON current becomes nearly constant after passing a certain critical doping. The tunneling probability depends on the tunneling width of the source/channel junction. A smaller tunneling width allows the electron to bridge the gap between the source valence band and channel conduction band (CB) easily. Increasing the source doping concentration is used as a method of decreasing the tunneling width by bringing the valence band and conduction band close together. As  $N_S$  is increased from  $8 \times 10^{18} \, \text{cm}^{-3}$  to  $5 \times 10^{19} \, \text{cm}^{-3}$  the tunneling width decreases and so the ON current will increase. However, as the concentration is increased to  $1 \times 10^{20} \, \text{cm}^{-3}$  there is not much movement of the bands. The tunneling width remains the same. Thus, the ON current is seen to be constant at higher doping. Fig. 4(b) shows dependence of  $I_{ON}$  on the VB effective mass. The  $I_{ON}$  predictably decreases with increase in  $m_v^*$ . The tunneling probability is proportional to the

exponential of the negative square root of the effective mass. A lower effective mass increases the tunneling probability and hence the ON current. A higher  $V_{DD}$  pushes down the conduction band further towards the valence band. Thus, the tunneling width is reduced and hence the effect of effective mass on the ON current somewhat reduces.

At low supply voltages, the on/off ratio follows a positive trend with increasing  $N_S$  and  $m_v^*$  as seen in Fig. 5(a) and (b). At low supply voltages the VB and CB are far apart. Thus, increasing doping decreases the tunneling width and a reduced effective mass enhances the tunneling probability. At higher voltages, the  $I_{ON}/I_{OFF}$  starts decreasing after reaching a critical doping concentration which is observed in Fig. 5(a). This happens because the OFF current increases with higher doping due to increased Auger generation rate but the ON current remains unchanged as the tunneling width remains fixed. The on/off ratio increases with increasing effective mass for higher supply voltages too as shown in Fig. 5(b). Another interesting observation from our simulation is that a SS < 60 mV/decade for four orders of magnitude of current is attained at higher supply voltages of 0.2 and 0.3 V even in the presence of Auger generation.

The subthreshold swing vs.  $I_{DS}$  for different carrier concentrations is shown in Fig. 6(a). We observe that lowering the concentration reduces the minimum SS. Reducing  $N_{\rm S}$  by an order of magnitude from  $1\times 10^{20}~{\rm cm}^{-3}$  to  $1\times 10^{19}~{\rm cm}^{-3}$  decreases the minimum SS from 21 mV/dec to  $15.82~{\rm mV/dec}$ . The effect of VB effective mass on SS is shown in Fig. 6(b). Increasing  $m_{\nu}^*$  shifts the curve downwards at low currents as seen in the plot. At  $I_{DS}=10^{-5}~{\rm \mu A/\mu m}$  increasing  $m_{\nu}^*$  from 0.043 to 0.103 decreases the SS from 42 mV/dec to 36 mV/dec. It has been previously shown that  ${\rm SS}_{Aug}\approx \frac{\mu^{-1}+1}{2\mu^{-1}+1}60~{\rm mV/dec}$  [18,23]. Here,  $\mu=m_c^*/m_{\nu}^*$ . This relationship explains why increasing VB effective mass can decrease the SS. A higher  $m_{\nu}^*$  reduces the mass ratio and thus leads to a decrease in the subthreshold swing.

Achieving subthreshold swing below 60 mV/dec will be immensely impactful for any device considered as a replacement for standard CMOS transistors. Our study acts as a reference for improving performance of TFETs and achieve SS < 60 mV/dec. The most effective way of reducing SS and improving the on/off ratio is by reducing the trap density. Often increasing carrier concentration is considered as a method of increasing ON current. However, as seen from our results this can be detrimental to TFET performance after a critical doping at high voltages, which must therefore limit the source doping. For further reduction of tunneling width other mechanisms like electrostatic doping can be used to enhance the ON current by placing an additional gate over the source region near the channel. In addition to doping the effective mass is also important for improving TFET performance. From our simulations we see that at high supply voltages, a slightly higher VB

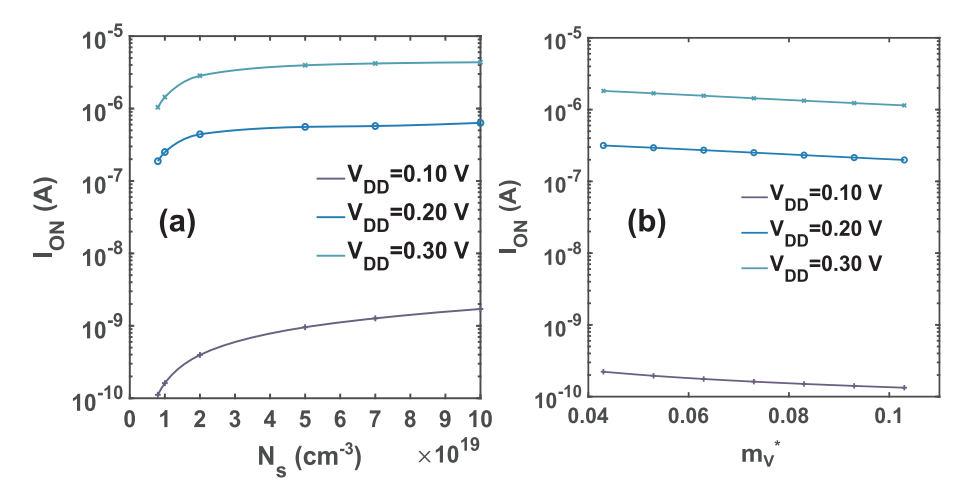


Fig. 4. ON current vs. (a) source carrier concentration (b) source valence band effective mass. The ON current only contains the contribution from Auger generation and ballistic processes, but not trap assisted tunneling.

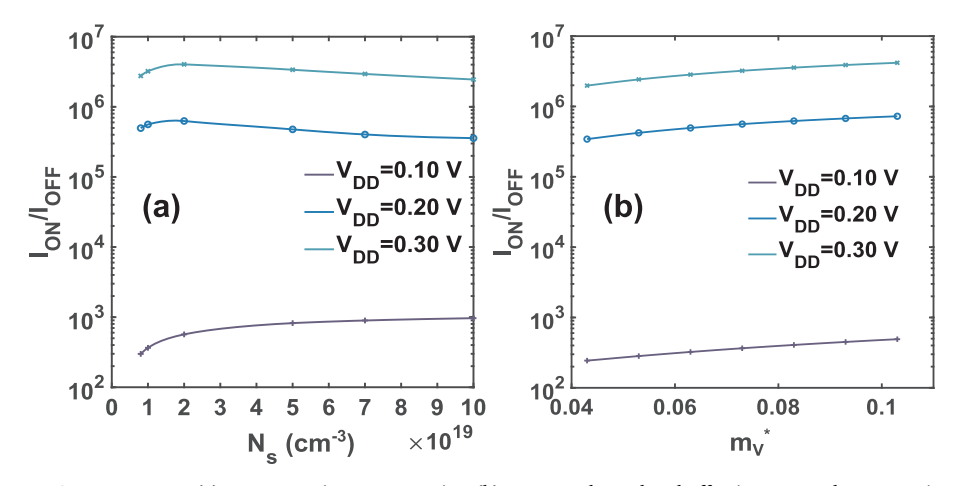


Fig. 5. Ratio of ON current to OFF current vs. (a) source carrier concentration (b) source valence band effective mass. The trap-assisted tunneling component is excluded from both the currents in order to study the effect of Auger generation on these.

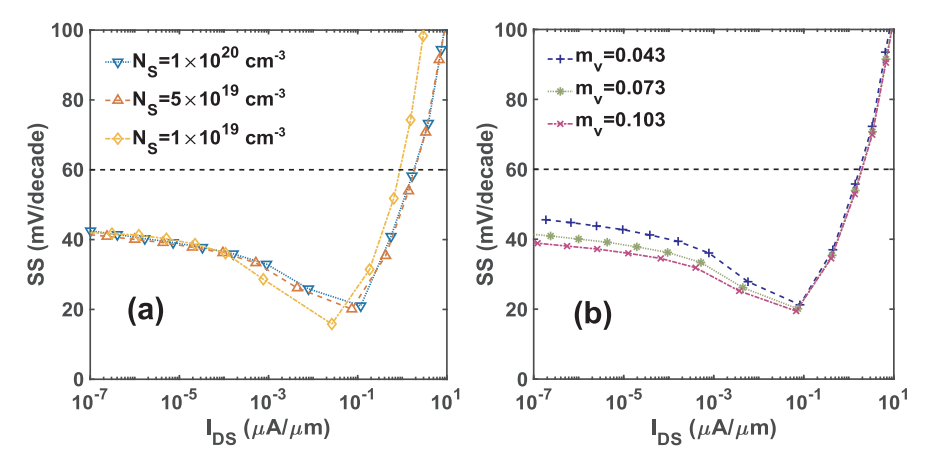


Fig. 6. SS vs. Auger(Auger + Ballistic) current for (a) different dopings (b) different effective mass.

effective mass can significantly reduce OFF current and improve on/off ratio without affecting the ON current. III-V tertiary and quaternary alloys can be studied for this purpose since changing their composition results in different properties.

### 4. Conclusion

We conclude from our simulations that the most significant leakage mechanism affecting TFET performance is TAT process. Improvement in device characteristics can be obtained by reducing trap density but even that does not take it to the ballistic regime, as the leakage current is dominated by Auger generation process at low trap densities. The device performance can be enhanced further by lowering the doping concentration and increasing source valence band effective mass in order to reduce Auger generation. To keep the ON current sufficiently high new device architectures like vertical Tunnel FETs [29] or the use of electrostatic doping can be explored to compensate for the lower doping.

## Acknowledgment

This work has been supported by the Semiconductor Research Corporation (Award 2694.02) and the National Science Foundation (Award 1640053).

## References

- Choi WY, Park BG, Lee JD, Liu TJK. Tunneling field-effect transistors (tfets) with subthreshold swing (ss) less than 60 mv/dec. IEEE Electron Device Lett 2007:28:743-5
- [2] Bernstein K, Cavin RK, Porod W, Seabaugh A, Welser J. Device and architecture outlook for beyond cmos switches. Proc IEEE 2010;98:2169–84.
- [3] Seabaugh AC, Zhang Q. Low-voltage tunnel transistors for beyond cmos logic. Proc IEEE 2010;98:2095–110.
- [4] Sajjad RN, Ghosh AW. Manipulating chiral transmission by gate geometry: switching in graphene with transmission gaps. ACS Nano 2013;7:9808–13.
- [5] Unluer D, Ghosh AW. Steep subthreshold switching with nanomechanical fet relays. IEEE Trans Electron Dev 2016;63:1681–8.
- [6] Shukla N, Thathachary AV, Agrawal A, Paik H, Aziz A, Schlom DG, Gupta SK, Engel-Herbert R, Datta S. A steep-slope transistor based on abrupt electronic phase transition. Nature Commun 2015;6:7812.
- [7] Khan AI, Yeung CW, Hu C, Salahuddin S. Ferroelectric negative capacitance mosfet: Capacitance tuning amp; antiferroelectric operation. 2011 International Electron Devices Meeting 2011. p. 11.3.1–4.
- [8] Appenzeller J, Lin Y-M, Knoch J, Avouris P. Band-to-band tunneling in carbon nanotube field-effect transistors. Phys. Rev. Lett. 2004;93:196805.
- [9] Sarkar D, Xie X, Liu W, Cao W, Kang J, Gong Y, Kraemer S, Ajayan PM, Banerjee K. A subthermionic tunnel field-effect transistor with an atomically thin channel. Nature 2015;526:91.
- [10] Lu H, Seabaugh A. Tunnel field-effect transistors: State-of-the-art. IEEE J Electron Devices Soc 2014;2:44–9.
- [11] Pandey R, Mookerjea S, Datta S. Opportunities and challenges of tunnel fets. IEEE Trans Circuits Systems I: Regular Papers 2016;63:2128–38.
- [12] Zhao X, Vardi A, del Alamo JA. Sub-thermal subthreshold characteristics in top?down ingaas/inas heterojunction vertical nanowire tunnel fets. IEEE Electron Device Lett 2017;38:855–8.
- [13] Memisevic E, Hellenbrand M, Lind E, Persson AR, Sant S, Schenk A, et al. Individual defects in inas/ingaassb/gasb nanowire tunnel field-effect transistors operating below 60 mv/decade. Nano Lett 2017;17:4373–80. https://doi.org/10.1021/acs.

- nanolett.7b01455. pMID: 28613894.
- [14] Memisevic E, Hellenbrand M, Lind E, Persson AR, Sant S, Schenk A, et al. Individual defects in inas/ingaassb/gasb nanowire tunnel field-effect transistors operating below 60 mv/decade. Nano Lett 2017;17:4373–80. https://doi.org/10.1021/acs. nanolett.7b0145. pMID: 28613894.
- [15] Vasen T, Ramvall P, Afzalian A, Doornbos G, Holland M, Thelander C, et al. Vertical gate-all-around nanowire gasb-inas core-shell n-type tunnel fets. Sci Rep 2019:9:202.
- [16] Sajjad RN, Chern W, Hoyt JL, Antoniadis DA. Trap assisted tunneling and its effect on subthreshold swing of tunnel fets. IEEE Trans Electron Devices 2016;63:4380–7.
- [17] Teherani JT, Chern W, Agarwal S, Hoyt JL, Antoniadis DA. A framework for generation and recombination in tunneling field-effect transistors. 2015 Fourth Berkeley Symposium on Energy Efficient Electronic Systems (E3S) 2015. p. 1–3.
- [18] Ahmed SZ, Tan Y, Truesdell DS, Calhoun BH, Ghosh AW. Modeling tunnel field effect transistors-from interface chemistry to non-idealities to circuit level performance. J Appl Phys 2018;124:154503 https://doi.org/10.1063/1.5044434.
- [19] Tan YP, Povolotskyi M, Kubis T, Boykin TB, Klimeck G. Tight-binding analysis of si and gaas ultrathin bodies with subatomic wave-function resolution. Phys Rev B 2015:92:085301
- [20] Tan Y, Povolotskyi M, Kubis T, Boykin TB, Klimeck G. Transferable tight-binding model for strained group iv and iii–v materials and heterostructures. Phys Rev B 2016;94:045311.
- [21] Simmons JG. Electric tunnel effect between dissimilar electrodes separated by a

- thin insulating film. J Appl Phys 1963;34:2581-90.
- [22] Sajjad RN, Antoniadis D. A compact model for tunnel fet for all operation regimes including trap assisted tunneling, in 2016 74th. 2016 74th Annual Device Research Conference (DRC) 2016. p. 1–2.
- [23] Teherani JT, Agarwal S, Chern W, Solomon PM, Yablonovitch E, Antoniadis DA. Auger generation as an intrinsic limit to tunneling field-effect transistor performance. J Appl Phys 2016;120:084507.
- [24] Dewey G, Chu-Kung B, Boardman J, Fastenau JM, Kavalieros J, Kotlyar R, et al. characterization, and physics of iii?v heterojunction tunneling field effect transistors (h-tfet) for steep sub-threshold swing. 2011 International Electron Devices Meeting. 2011. p. 33.6.1–33.6.4..
- [25] Baik M, Kang H-K, Kang Y-S, Jeong K-S, Lee C, Kim H, et al. Effects of thermal and electrical stress on defect generation in inas metal oxide semiconductor capacitor. Appl Surface Sci 2019;467-468:1161–9.
- [26] Neophytou N, Paul A, Klimeck G. Bandstructure effects in silicon nanowire hole transport. IEEE Trans Nanotechnol 2008;7:710–9.
- [27] Klimeck G, Bowen RC, Boykin TB. Strong wavevector dependence of hole transport in heterostructures. Superlattices Microstruct 2001;29:187–216.
- [28] Long P, Huang JZ, Povolotskyi M, Klimeck G, Rodwell MJW. High-current tunneling fets with (*bar1*0) orientation and a channel heterojunction. IEEE Electron Device Lett 2016;37:345–8.
- [29] Jena D. Tunneling transistors based on graphene and 2-d crystals. Proc IEEE 2013;101:1585–602.